HAIT Journal of Science and Engineering B, Volume 2, Issues 5-6, pp. 762-775

A new application of power electronics: the ion thruster HV drive

Federico Belloni*, Piero G. Maranesi, and Marco Riva

Sezione Elettronica, Università degli Studi di Milano
Via Celoria 16, 20133 Milano, Italy
**Corresponding author: federico.belloni@unimi.it*

Received 1 March 2005, accepted 7 June 2005

Abstract

The paper addresses the high voltage drive for ionic motors on board of satellites. A modular solution for HV generators driving the radio-frequency ion thrusters is proposed taking into account the peculiarities of the plasma load. The dynamic characteristics of the HV power cells are described all over their operating ranges. Analytic results and computer simulations show suitability of the devices for reaching sufficient stability margins through appropriate feedback.

Keywords: Spacecrafts propulsion, ion thrusters, high voltage generators

1 Introduction

Until now, controlled hydrazine jets were generally used for the propulsion, orbit control, and orientation of the space vehicles after their launch to orbit. In the last years, a new class of thrusters, based on electrical energy conversion, has been proposed and tested on board. In these engines an ionized gas is accelerated using electrical energy and expanded through a nozzle. Such systems can eject ions at an exhaust velocity v_e which is an order of magnitude higher than that of hydrazine or other chemical propellants. So, a larger thrust, $T = d(mv)/dt = \dot{m}v_e$, and speed variation $\Delta v = v_e ln(m_o/m_f)$ can be reached, being m_o and m_f the initial and final mass of the satellite [1, 2].

Two categories of ion thruster have been developed:

- electrostatic propulsors, wherein plasma is accelerated by an electric field
- electro-magnetic propulsors, wherein plasma interacts also with an internal or external magnetic field.

Each category includes different types of engines whose power spans over a range from tens of watts to several tens of kilowatts.

This paper makes reference to one of most promising motors, the Radio-frequency Ion Thruster (RIT). Accelerating forces of the order of several tens of millinewtons can be obtained with few kilowatt RITs well suited for interplanetary missions. Their schematic structure is shown in Fig. 1 [3–8].

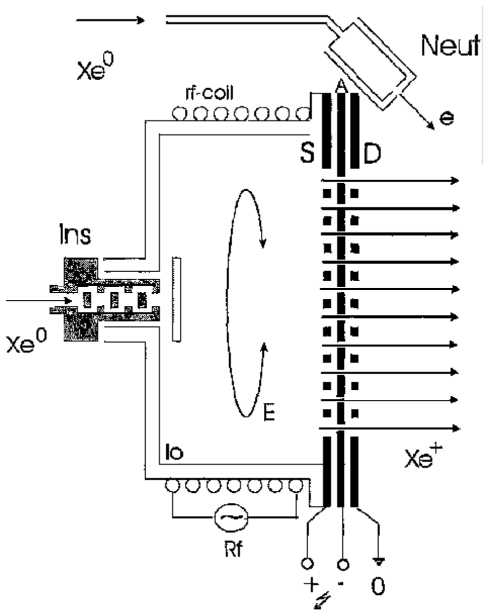

Figure 1: Scheme of a radio-frequency ion thruster.

The used propellant is an inert gas, such as argon, krypton or, most commonly, xenon ionized by a radio-frequency generator and then accelerated by a couple of high voltage grids. The first grid (beam grid) is maintained at a positive voltage and the second one (extraction grid) at a negative voltage. The propellant is sent, through an insulating valve, into a cylindrical discharge chamber. This chamber is inductively coupled with a radio-frequency source (frequency of a few MHz) that provides the power for ionization of the propellant. After striking the plasma, the electrical discharge is self-sustained by the electrons produced by gas ionization. The ions with kinetic energy high enough to overpass the barrier of the positive grid, flow out accelerated by the electric field. An equal amount of plasma electrons is collected by the grid; the rate of such charge is the load current of the Positive High Voltage Generator (PHVG) closed by the electrons from the external neutralizer. The electron emission, improved by thermo-ionic effect, ensures the charge balance. The negative downstream grid prevents the back streaming of electrons.

The exhaust velocity is $v_e = (\frac{2q_i V_{bg}}{m_i})^{\frac{1}{2}}$ where V_{bg} is the voltage of beam grid, q_i and m_i are, respectively, the charge and the mass of a single positive ion [1]. Due to the threshold effect of the positive grid, the beam current (I_{beam}) decreases by increasing the voltage ($dI_{beam}/dV_{bg} < 0$), that is a negative resistance behaviour.

In any case it exists an optimal power operating point ($V_{bg,opt}$) for the PHVG. 1.5kV is around the optimal value for RITs in the range of a few kilowatts.

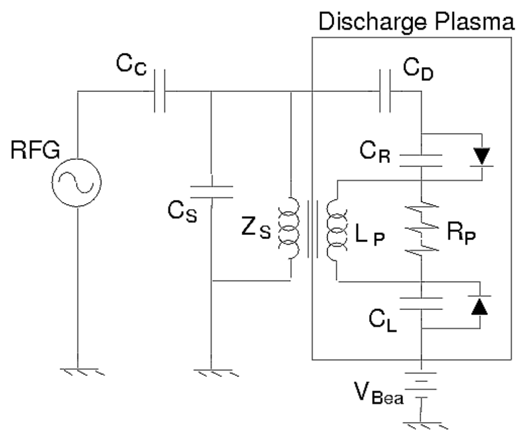

Figure 2: Equivalent electric model of the RIT seen from the radio-frequency generator.

The negative resistance behaviour is not the only peculiarity of the load of the PHVG. In fact the plasma behaves as a non-linear load as it can be deduced from the Fig. 2 which shows the equivalent circuit seen by the

Radio-frequency Generator.

V_{Beam} is the plasma beam potential given by the sum of the sheath potential with the voltage of the positive grid. The sheath potential is in the order of a few tens of volts and represents the voltage drop from the outer portion of the plasma to the inner one. It is due to the internal dynamics of charged particles interacting with the electric field of the beam grid [9].

Short circuit between the positive and the negative voltage grids happens not rarely and capability to withstand such an event is mandatory.

From this concise description, the requirement of adopting a robust high voltage generator suited for negative resistance non-linear loads emerges.

2 A proposal for the high voltage drive

To satisfy the requirement, the high voltage power cell should have an elementary dynamic behaviour providing current to its output capacitance and load as a pure transconductance driven by the control voltage V_C: $I_{beam} = I_{out} = g_m V_C$.

Even if g_m is not constant, such a dependence provides degrees of freedom in the assignment of some kind of time-invariant feedback avoiding complicated adaptive control solutions.

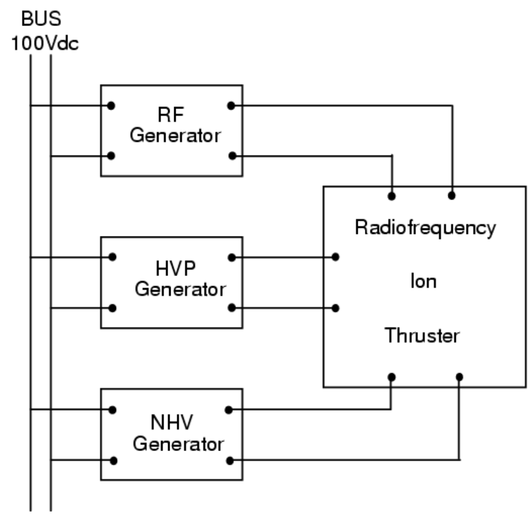

Figure 3: Block scheme of the voltage generators assembly.

To cope with different characteristics of the load, in terms of rated power, optimal voltage, equivalent load circuit related to the chosen propellant, etc., it looks worth addressing the design to a modular circuit characterised by parallelability. Hence pure transconductance control of output current transmission and parallelability are the characteristics of the ideal modular high voltage generator whose optimal power size has been estimated around 1.5kW and output voltage around 1.5kV.

The power generator set up is shown in Fig. 3.

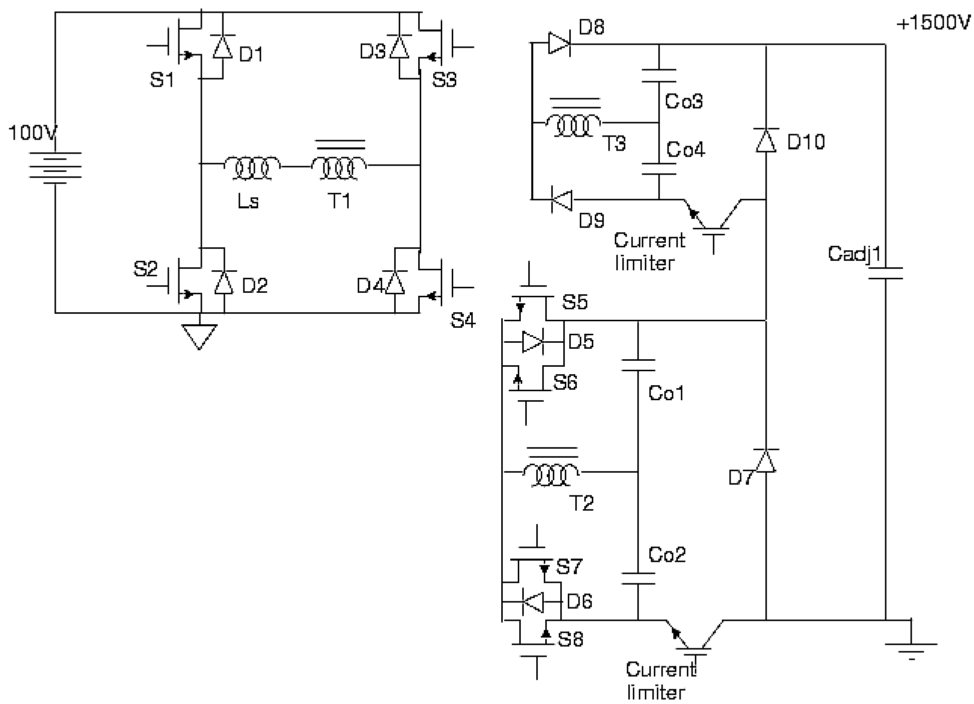

Figure 4: The phase-shift controlled step-up converter for the positive HV generator.

The proposed solution for the PHVG finds some forerunners in [10–12]. It is shown in Fig. 4 representing a phase-shift controlled converter switching at the frequency of $1/T = 65.5$kHz. The input voltage is the 100V DC bus, the output is provided by a series of two 750V secondary windings, the former is rectified by active switches, the latter by diodes in the half bridge connection. Zero voltage switch-on and voltage clamping characterize the switching transients. The IGBTs, in series to the output, avoid to overcome the load current limit in the cases of short circuit or fast rising overcurrent.

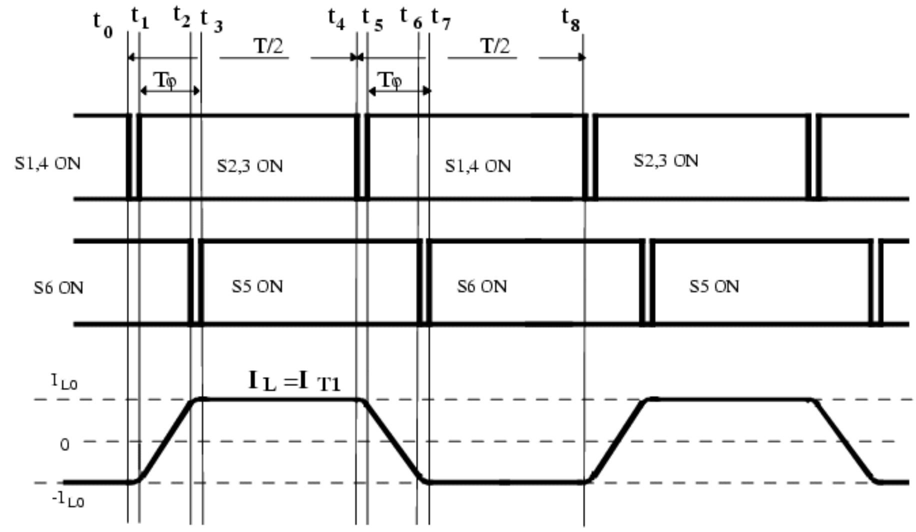

Figure 5: Switching commands and inductor current waveforms of the PHVG.

In Fig. 5 the main waveforms describing the steady state operation are reported. The current in the primary transformer and in the inductor L depends on the phase-shift T_φ from the switching commands in the full bridge and those in the active secondary side half bridge.

The transformer winding ratio $n = n_2/n_1 = n_3/n_1$ is a quarter of the output to input voltage ratio.

When S5 goes on at the end of T_φ ($t = t_3$), I_L reachs its maximum and remains constant until the diagonal switches S2 and S3 are on because the voltage across L is null: $V_L = V_{IN} - V_{OUT}/(4n) = 0$. Diode D8 is on as well, and the current I_L/n is injected to the output nodes from t_3 to t_4.

When S1 and S4 go on ($t = t_5$), the voltage of the primary transformer remains unchanged sustained by the output voltage $V_{OUT}/4$ of the active half bridge. The voltage across L drops to $-2V_{IN} = -V_{IN} - V_{OUT}/(4n)$. The transformer current is reversed and reaches its highest negative value after a delay time T_φ when the switch S5 goes off and S6 turns on ($t = t_7$). At the same time, the diode D9 switches on and a situation symmetrical to that of the time slot t_3 - t_4 repeats in the time slot t_7 - t_8.

During the switching delays from turn off to turn on (t_0 - t_1, t_2 - t_3, t_4 - t_5, t_6 - t_7), the transients are driven by the inductor current I_L until natural switch-on of the intrinsic MOS body diodes clamp the voltage ensuring zero voltage switch-on.

Neglecting the parasitic effects, the output power is given by:

$$P_{OUT} = 2\frac{V_{IN}^2 T_\varphi}{LT}\left(\frac{T}{2} - T_\varphi\right).$$

Its dependence on T_φ is represented in Fig. 6.

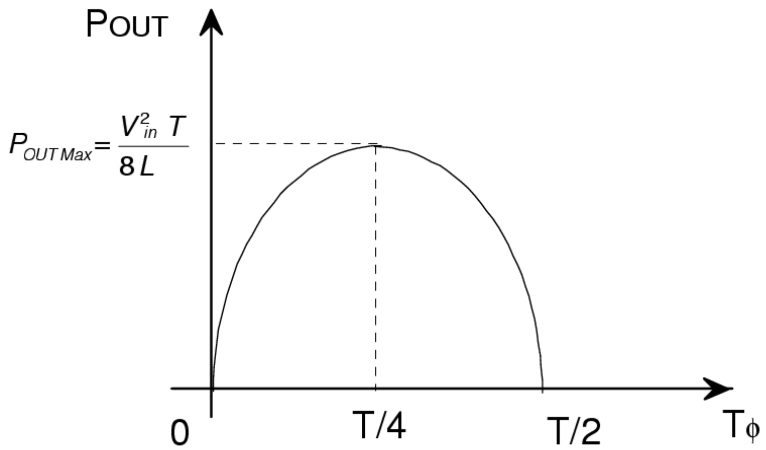

Figure 6: Output power versus phase-shift time.

The control variable T_φ is allowed to span from 0 to T/4 and within this range a linear small signal model can be deduced. It is reported in Fig. 7.

The solution for the control to output transfer function takes the form: $v_{out}/v_c = \alpha/(1 + s\tau)$ that well fits the ideal behavior $v_{out}/v_c = g_m/(sCout)$ mentioned before, even though α depends on the operating conditions and expresses the non-linearity of the large signal overall dynamics.

A better approximation in the forecasts has been reached through simulations performed by FREDOMSIM which is a software tool that automatically provides the small signal characterizations of switching PWM controlled networks [13, 14]. This tool uses PSpice models of the electronic devices and it improves the forecasts built on the assumption of ideal components.

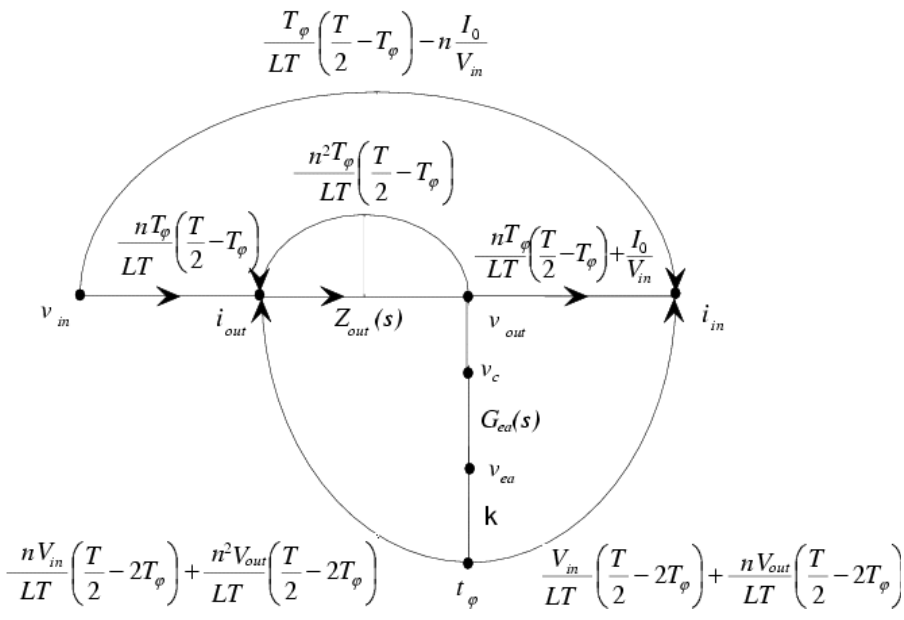

Figure 7: Flow-chart of the converter small signal dynamics; k is the control voltage to phase-shift time conversion constant.

The simulated gain and phase frequency responses of the control to output transfer function are plotted in Fig. 8 relevant to two different operating points: maximum load current (1A) and reduced load current (0.5A). A confirmation of the first order dynamic behavior transpires.

The control optimization of the high voltage generator supplying an ion thruster has to take into account the overall system non-linearity and the peculiarities of the load. Anyway, it seems that the dynamic performances of the power cell approach the ideal characteristics and open up the solution of the problem by means of classical feedback techniques and time-invariant networks.

A similar topology has already been adopted for the 120V to 28V DC-DC converter employed on board the International Space Station (ISS) for non-US loads and realized by Carlo Gavazzi Space s.p.a.[15].

The experimental measurements on this step-down DC to DC converter demonstrated a good compliance of the dynamic forecasts with the real life. It is worth remarking that the same type of dynamic flow chart shown in Fig. 7 holds for the ISS converter that typically supplies a number of payload DC to DC converters characterised by negative input resistance [12].

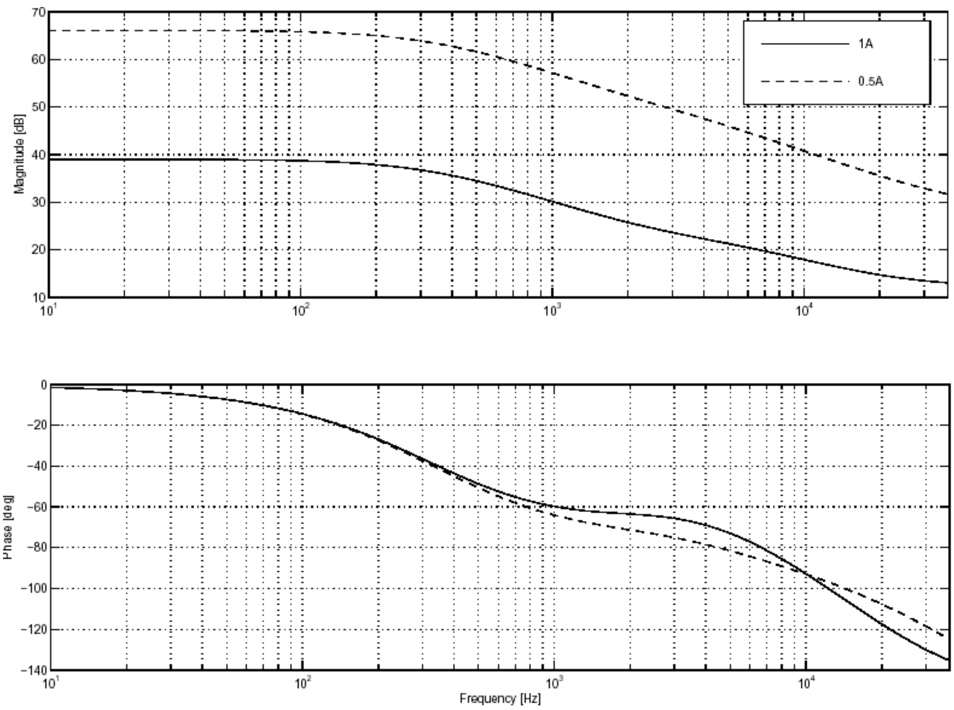

Figure 8: Gain and phase frequency responses of the control to output transfer function for the PHVG.

The power supply assembly of the RIT is completed by the Negative High Voltage Generator (NHVG) for the negative grid. This converter has to supply a voltage from -100V to -800V with a maximum current of a few hundreds milliamperes corresponding to the rate of positive ions trapped by the grid.

The modular approach is not suited for the NHVG. In fact, a power capability of 300W satisfies the RIT drive exigencies of ionic motor up to several kilowatts.

The complex dependence of the load current on the supply voltage that has been remarked in the case of PHVG does not hold the same way for the NHVG. Nevertheless, it is worth characterizing also the negative grid voltage supply with a first order dynamics and with full-control cycle-by-cycle of the charge injected to the load. This last quality turns out useful in the design of the control system and in facing the short circuits between the positive and negative grids.

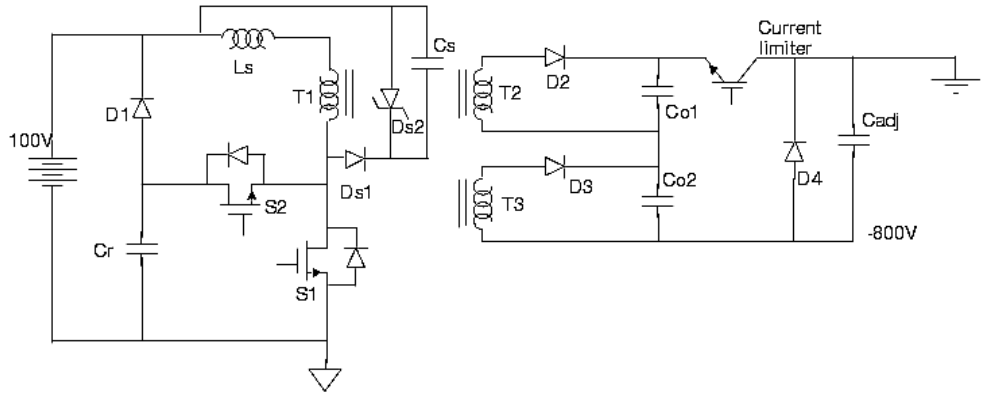

Figure 9: Soft-switched flyback converter in the DCM for the negative HV generator.

A flyback topology in the discontinuous conduction mode, switching at the frequency of 65.5kHz, provides such performances and it has been selected for the power cell implementation. As shown in Fig. 9, a soft-switching configuration has been adopted to maximize the efficiency. Forecasts of the small signal dynamics of the NHVG has been done by FREDOMSIM. Plots of the control to output frequency responses are reported in Fig. 10. They are referred to an output voltage of -800V and two different load currents of 375mA and 100mA.

Parameters and device specifications relevant to the prototype of the circuits in the Figs. 4 and 9 are given in the Tables 1 and 2.

L	11.1μF
Cout	1μF
$n = n_2/n_1 = n_3/n_1$	3.75
S1, S2, S3, S4	Irhna57163se
S5, S6	Irfpg50
D8, D9	MUR4100
D7, D10	MUR4100
IGBT	Irg4ph50s

Table 1: PHVG specifications.

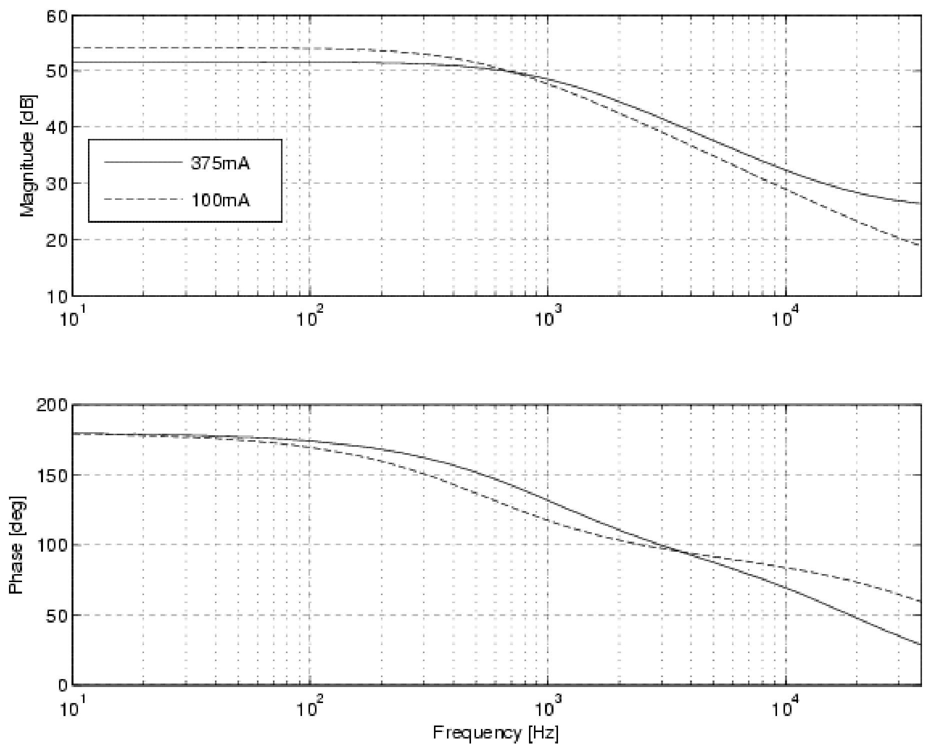

Figure 10: Gain and phase frequency responses of the control to output transfer function for the NHVG.

3 Conclusions

A solution to the problem of driving RIT ionic motors for space applications has been presented and justified.

- A modular set up has been chosen for the Positive High Voltage Generator (PHVG).
- The modules can be connected in parallel and they are sized 1.5kW each. This allows us to conveniently satisfy the high voltage drive requirements in the range from 1kW to 6kW wherein the RIT motors are presumed to be applied most frequently.
- The selected topology of the PHVG power cell is a phase-shifted dual-active converter characterized by a full bridge primary side and two

Ls	400nH
Cr	4nF
Cs	1μF
Cout	100nF
$n = n_2/n_1 = n_3/n_1$	4
S1	Irhm7360se
S2	Irhna57163se
D1	ES3G
Ds1	ES3G
Ds2	BZV90C30
D2, D3	BYW96E
D4	MUR4100
IGBT	Irg4ph50s

Table 2: NHVG specifications.

half bridge rectified secondary sides. These last are connected in series, the former is active and uses MOS switches, the latter is rectified by diodes.

- The control voltage fully determines cycle-by-cycle the charge injected to the load; hence the output current is controlled within a single switching period from zero to its maximum.

- In the linear approximation the power cell has a first order dynamics even though the transconductance di_{out}/dv_c is non-linear and depends on the output power. The characteristics of the PHVG simplify the control. The control optimisation has to face the non-linearity and negative resistance behaviour of the plasma load, anyway.

- The high voltage supply of the negative grid is based upon a soft-switched flyback cell operating in the discontinuous conduction mode. Even though this generator is less critical than that applied to the positive grid, its dynamic characterisation is similar to that of the PHVG and well suited to stand short circuits between the grids.

Carlo Gavazzi Space s.p.a., Via Gallarate 150, 20151 Milano, Italy, has supported the design of the described converters and made its R&D lab available for realizing a prototype and testing it. The authors also acknowledge the contributions of Roberto Grossi and Stefano Chiesa.

References

[1] R.G. Jahn and E.Y. Choueiri, In: *Encyclopaedia of Physical Science and Technology*, Ed.: R.A. Myers, 3rd ed., vol. **5**, p. 125 (Academic Press, San Diego, 2002).

[2] H. Bassner, R. Killinger, H. Leiter, and J. Mueller, 37th AIAA/ASME/SAE/ASEE Joint Propulsion Conference and Exhibit, Salt Lake City, Utah, 8-11 July 2001.

[3] M. Zeuner, F. Scholze, H.J. Leiter, R. Kukies, D. Feili, M. Tartz, and H. Neumann, 39th AIAA/ASME/SAE/ASEE Joint Propulsion Conference and Exhibit, Huntsville, Alabama, 20-23 July 2003.

[4] M. Zeuner, F. Scholze, H.J. Leiter, R. Kukies, D. Feili, M. Tartz, and H. Neumann, 39th AIAA/ASME/SAE/ASEE Joint Propulsion Conference and Exhibit, Huntsville, Alabama, 20-23 July 2003.

[5] R. Killinger, H. Bassner, and J. Mueller, 35th AIAA/ASME/SAE/ASEE Joint Propulsion Conference and Exhibit, Los Angeles, California, 20-24 June 1999.

[6] S. Kitamura, K. Miyazaki, Y. Hayakawa, H. Yoshida, and K. Akai, *Performance improvement of 150-mN xenon ion thrusters*, based on paper IAF-98-S.4.10 presented at the 49th International Astronautical Congress, Melbourne, Australia, 28 September-20 October 1998.

[7] Louis R. Piñero, *Design of a Modular 5-kW Power Processing Unit for the Next-Generation 40-cm Ion Engine*, presented at the 27th International Electric Propulsion Conference, Pasadena, California, 15-19 October 2001.

[8] M. Zeuner, F. Scholze, H.J. Leiter, R. Kuies, D. Feili, M. Tartz, and H. Neumann, 39th AIAA/ASME/SAE/ASEE Joint Propulsion Conference and Exhibit, Huntsville, Alabama, 20-23 July 2003.

[9] M. Zeuner, F. Scholze, B. Dathe, and H. Neumann, Surface and Coatings Technology 2001, p.39 (2001).

[10] M.H. Kheraluwala, R.W. DeDoncker, and D.M. Divan, Proceedings of the EPE Conference '91, p. 551 (1991).

[11] P. Maranesi, Proceedings of the IEEE-PESC '93, Seattle, p. 185 (1993).

[12] F. Belloni, P. Maranesi, and M. Riva, Proceedings of the EPE Conference '03, Toulouse, France, 2 - 4 September 2003.

[13] P. Maranesi, IEEE Trans. Power Electronics **7**, 83 (1992).

[14] P.G. Maranesi and M. Riva, IEEE Power Electronics Letters **1**, 97 (2003).

[15] A. Lamantia, P. Maranesi, and G. Sablich, Proceedings of the ESPC '98, Tarragona, Spain, 21 - 25 September, vol.**1**, p. 219 (1998).